ORIGINAL ARTICLE

Combined blockade of TGf-β1 and GM-CSF improves chemotherapeutic effects for pancreatic cancer by modulating tumor microenvironment

Qiaofei Liu[1,3,4] · Huanwen Wu[2,3,4] · Yuan Li[2,3,4] · Ronghua Zhang[1,3,4] · Jorg Kleeff[5] · Xiang Zhang[1,3,4] · Ming Cui[1,3,4] · Jingkai Liu[1,3,4] · Tong Li[1,3,4] · Junyi Gao[1,3,4] · Boju Pan[2,3,4] · Wenming Wu[1,3,4] · Weibin Wang[1,3,4] · Li Zhou[1,3,4] · Junchao Guo[1,3,4] · Menghua Dai[1,3,4] · Taiping Zhang[1,3,4] · Quan Liao[1,3,4] · Zhaohui Lu[2,3,4] · Yupei Zhao[1,3,4]

Abstract

The interactions between tumor immune microenvironment (TIME) and pancreatic cancer cells can affect chemotherapeutic efficacy; however, the mechanisms still remain largely unknown. Thirty items in TIME were comprehensively screened by using tissue microarray from pancreatic cancer patients. Their expressions, interconnections and predictive roles for survival were analyzed. Twenty-one of 30 items could stratify the survival of the patients; however, multivariate analysis found that only 5 independent risk factors could predict worse survival (M2-polarized tumor-associated macrophages (TAMs), IgG4 positive cells, TGF-β1, GM-CSF and lymphangiogenesis). They had a much higher expression levels in tumoral tissue, compared to peritumoral tissue. The Spearman analysis showed that M2-polarized TAM, TGF-β1 and GM-CSF were positively correlated with pancreatic cancer stem cells (PCSC), angiogenesis and lymphangiogenesis. Both human and murine pancreatic cancer cells could induce M2-polarized TAM, which showed substantial roles to decease chemotherapeutic effects. After treated by gemcitabine, both human and murine pancreatic cancer cell lines expressed higher level of immune check points, PCSC markers and varieties of immunosuppressive factors; however, TGF-β1 and GM-CSF had the highest increase. Based on the above results, TGF-β1 and GM-CSF were proposed to be the optimal potential targets to improve chemotherapeutic effects. In immunocompetent murine models, we demonstrated that combined blockade of TGF-β1 and GM-CSF improved the chemotherapeutic effects by inhibition of M2-polarized TAM and induction of CD8 positive T cells. This study presents a novel promising combined strategy to improve the chemotherapeutic effects for pancreatic cancer.

Keywords Pancreatic cancer · Tumor immune microenvironment · Chemotherapy · Tumor-associated macrophages · TGF-β1 · GM-CSF

Qiaofei Liu, Huanwen Wu, Yuan Li and Ronghua Zhang have contributed equally to this work.

✉ Quan Liao
  lqpumc@126.com

✉ Zhaohui Lu
  path2008@163.com

✉ Yupei Zhao
  zhao8028@263.net

Extended author information available on the last page of the article

Abbreviations

ACT	Adjuvant chemotherapy
ARG1	Arginase1
CSF	Colony stimulating factor
CTL	Cytotoxic T lymphocytes
Gem	Gemcitabine
GM/M-CSF	Granulocyte macrophage/macrophage colony stimulating factor
IFN-γ	Interferon-γ
IL	Interleukin
iNOS	Inducible nitric oxide synthase
LPS	Lipopolysaccharides
MDSC	Myeloid-derived suppressor cells
MLVD	Microlymphatic vascular density
MVD	Microvascular density
PCSC	Pancreatic cancer stem cells

PDAC   Pancreatic ductal adenocarcinoma
PD-1   Programmed death 1
PDL-1   Programmed death ligand-1
STAT   Signal transducer and activator of
            transcription
TAM   Tumor-associated macrophages
TGF-β1   Transforming growth factor beta-1
Th1/2   T helper 1/2
TIME   Tumor immune microenvironment
TNF-α   Tumor necrosis factor-α
Treg   Regulatory T cells
VEGF   Vascular endothelial growth factor

Introduction

Pancreatic ductal adenocarcinoma (PDAC), accounting for more than 80% of pancreatic cancer, is one of the most deadly malignant tumors [1, 2]. Even for the patients with early stage of PDAC, the overall 5-year survival rate is only 40% [3]. Adjuvant chemotherapy treatment (ACT) has been demonstrated to improve the survival of the patients, and it is recommended for any stage of PDAC [3]. Gemcitabine (GEM) is the most widely used drug for ACT; however, the response rate remains low. Since GEM plus capecitabine or FOLFIRINOX (oxaliplatin, leucovorin, irinotecan and 5-FU) improved median and overall survival compared to GEM alone [4], development of new strategies to improve the efficacy of chemotherapy is still of great importance.

PDAC has a peculiar tumor immune microenvironment (TIME), characterized by extensive desmoplasia and abundant infiltration of immune cells [5, 6]. Cancer cells produce various factors to expand, induce or suppress immune cells [7]. At the initial stage of pancreatic carcinogenesis, there is an accumulating infiltration of immunosuppressive cells, such as myeloid-derived suppressor cells (MDSC), regulatory T cells (Treg) and tumor-associated macrophages (TAMs) [8, 9]. Clinically, more infiltration of these immunosuppressive cells in tumor tissue predicts poor survival of pancreatic cancer patients [8, 10, 11]. TAM has two polarized types, M1 and M2, which exert different or even opposite roles in inhibiting or promoting cancer cells [12, 13]. Activation of TAM by CD40 improved the effects of GEM in a murine model [14]. Although the interactions between cancer cells and immune cells have drawn increasing concerns, the landscape of TIME of PDAC patients has not been comprehensively analyzed before.

Chemotherapeutic resistance and distant metastasis are two main causes of death caused by PDAC. The PCSC is the most drug-resistance subpopulation of cancer cells [15]. Angiogenesis and lymphangiogenesis contribute to metastasis of cancer cells. Herein, 30 markers of five important aspects, including cancer stemness, angiogenesis, lymphangiogenesis, immune cells and immune regulatory factors (Th1/Th2 cytokines, GM/M-CSF, transforming growth factor -β1(TGF-β1), tumor necrosis factor-α (TNF-α), interferon-γ (IFN-γ) and immune check points) produced by cancer cells were analyzed to depict the landscape of TIME of PDAC, and their interconnections and predictive roles for the efficacy of GEM were further explored.

Chemotherapeutic drugs can induce immunogenic death of cancer cells to activate anti-tumor responses and even directly kill certain immunosuppressive cells; however, they can also stimulate cancer cells to release immune regulatory factors to remodel a more immunosuppressive TIME [3, 11, 16]. In this study, the remodeling effects and mechanisms of GEM on TIME of PDAC were also studied, which may lead to drug resistance.

Based on the systematical analysis of the landscape of the TIME of PDAC patients and its reciprocal interactions with chemotherapy, the potential targets in TIME to improve the efficacy of GEM were proposed according to the following criteria: (1) high level of expression in tumor tissues, no or low-level of expression in peritumoral tissues; (2) independent risk factor for worse survival; (3) correlation with cancer stemness, angiogenesis or lymphangiogenesis; (4) elevated expression after GEM treatment, which may lead to drug resistance.

These potential optimal targets were validated in immunocompetent murine pancreatic cancer models. This study found that combined blockade of TGF-β1 and GM-CSF was a potential promising new regimen to improve the efficacy of GEM by modulation of the TIME of PDAC.

Methods and materials

Patients and follow-up

Ninety-seven cases of patients with PDAC were successively enrolled following the inclusion criteria: (1) informed consent for sample donation for research use was obtained; (2) no neoadjuvant treatment was performed; (3) PDAC was pathologically confirmed; (4) R0 pancreaticoduodenectomy (tumor margin > 1 mm) was achieved; (5) tumor tissue and peritumoral tumor tissue were obtained; (6) at least three months of GEM-based ACT was performed; (7) information of postoperative survival time and the cause of death were available. Patients with any kind of autoimmune diseases were excluded. Sixteen clinicopathological characters were documented, including sex, age, differentiation grade, lymph node metastasis, tumor size, perineural invision (PIN), microcancerous embolus, the 8th TNM staging, serum CA 19-9, CA 242, CEA, neutrophil-to-lymphocyte ratio (NLR), platelet-to-lymphocyte ratio (PLR), diabetes and preoperative bile drainage. After surgery, patients were followed up

every 3 months by outpatient clinic or telephone interview, until the death of the patients or the end of this study. The overall survival time (OS) was recorded.

Tissue microarray construction

Tissue microarrays (TMA) were constructed using formalin-fixed paraffin-embedded blocks and the Mitogen MiniCore system. Ninety-seven samples from PDAC patients were reviewed by hematoxylin–eosin staining, and the representative areas were marked in distance from secondary necrotic and hemorrhagic fields. Four 2-mm-diameter cylinders of each case from two different areas of tumoral and peritumoral region were made (totally, 388 cores).

Immunohistochemical staining (IHC) and scoring

The landscape of TIME of PDAC was depicted by evaluation of 30 items from 5 aspects, including 14 immune cell markers, 11 immune regulatory markers (Th1/Th2 cytokines, GM/M-CSF, TGF-β1-IFN-γ-TNF-α-PDL1), 2 pancreatic cancer stem cell markers (PCSC) and 2 angiogenesis and lymphangiogenesis markers. Immunohistochemical staining was routinely performed, as previously reported [8]. The information of different primary antibodies was presented in supplementary material (Table S1). Staining was analyzed by two experienced pathologists (Huanwen Wu and Yuan Li) blinded to patient data, using a computerized image analysis system.

Firstly, under low power view, 6 areas with abundant infiltration of immune cells were selected in each tissue core by each pathologist, and the positive immune cells were stained to be brown and then these positive stained cells were counted under 400× magnification. The average count/HFP from the total number of two pathologists was counted. The average count/HPF of 0–4/HPF, 5–10/HPF and > 10/HPF was defined as low, moderate and high level of infiltration, respectively [10, 17](Fig. S1).

To score immune regulatory factors expressed in cancer cells, the positive ratio of cancer cells was classified into five grades (0: 0–5%; 1: 6%-25%; 2: 26%-50%; 3: 51% to 75%; 4: 76% to 100%), and the staining density was classified into four grades (0: negative; 1: weak; 2: moderate; 3: strong staining), and the average value calculated as ratio×intensity of two pathologists. The final score of 0–4, 5–8 and 9–12 was defined to be negative/weak, moderate and strong expression, respectively [18] (Figs. S2–S4).

A ratio of CD133 or ALDH1A positive cancer cells > 5% was defined as PCSC positive (Fig. S5). The CD34 and D2-40 were used to mark angiogenesis and lymphangiogenesis, respectively. Microvessels were defined as vessels with a clearly defined lumen or a well-defined linear vessel shape or a CD34 (vascular vessel) or D2-40 (lymphatic vessel) positive cell cluster consisting of more than 3 cells. Referring to the similar scoring method of immune cells, the microvascular density (MVD) and microlymphatic vessel density (MLVD) were counted, under 200× magnification (Fig. S6).

Determination of the optimal cutoff values for prediction of OS of the PDAC patients

The software X-tile has been widely used to determine the optimal cutoff values for prediction of prognosis [19]. In this study, we adopted X-tile to determine the optimal cutoff value to predict OS when the minimal *p* value was met (Fig. S7).

Immunocompetent mice

Male 4-week-old or 8-week-old C57BL/6 J mice were used. All animals were maintained in a specific pathogen-free animal facility.

Human or murine PDAC cell lines and monocyte/macrophage cell lines

One murine PDAC cell line (Panc02) and three human PDAC cell lines (T3M4, Mia PaCa-2 and PANC-1) were used and maintained in high glucose DMEM (Dulbecco's modified Eagle medium; Gibco BRL Co. Ltd., USA) supplemented with 10% FCS (fetal calf serum; Gibco BRL Co. Ltd., USA) and 1% penicillin and streptomycin.

Murine RAW 264.7 monocyte cell line and human THP-1 monocyte cell line were used. The RAW 264.7 cells were maintained in DMEM, and the THP-1 cells were maintained in RPMI-1640 medium (Sigma-Aldrich, Saint Louis, USA).

Carboxyfluorescein succinimidyl amino ester (CFSE) labeling of human or murine macrophages

The CFSE (Sigma-Aldrich, Saint Louis, USA) was used for alive cell labeling. Cell suspension of macrophages was diluted into 10^7/ml, and the CFES/DMSO (Sigma-Aldrich, Saint Louis, USA) solution was added. The final working solution of CFSE was 2.5 μmol/l 30 min later, cell culture medium with 10% FCS was added to stop the reaction, followed by washing. The changes of morphology of macrophages were observed under fluorescence microscope.

Generation of human or murine PDAC-induced TAM from different origins

The murine bone marrow cells were harvested from femur of 4-week-old C57 mice, and bone marrow derived macrophages (BMDM) were induced by 40 ng/ml M-CSF

(Sigma-Aldrich, Saint Louis, USA) for 4 days. The murine Panc02 PDAC cells were co-cultured with murine macrophages (RAW264.7 or BMDM) for 48 h through the transwell coculture system to induce murine BMDM-derived TAM. Human monocyte cells (THP-1) were induced into naïve macrophages (M_φ group) by using phorbol-12-myristate-13-acetate (PMA; 100 ng/mL) for 24 h. Human PDAC cells were co-cultured with M_φ for 48 h through the transwell coculture system to induce human TAM.

The PDAC cells were removed, and the co-cultured TAMs were washed with PBS three times. Then, the TAMs were cultured for another 48 h and the supernatant (SN) of human or murine PDAC-induced TAM was collected for further study. The SN from PDAC-induced TAM or naïve macrophages was added to make 20% or 40% conditional culture medium, respectively.

Chemotherapy in vitro

The different concentrations of GEM (Eli Lilly and Company, Indianapolis, USA) were used to treat different human and murine PDAC cells under different conditional culture media for 48 h. Then, the apoptosis and death of cancer cells were detected by PI/Annexin V-FITC methods, according to the manufacturer's protocol (NEOBIOSCIENCE, Shenzhen, China). Each experiment was performed three times.

Flow cytometry (FCM)

The subcutaneous tumor was harvested by blunt dissection and then cut into small pieces and minced using blades. Then, the minced pieces were digested with 200U/mL collagenase IV (Sigma-Aldrich, USA) and incubated at 37 °C for 1.5 h. Then, the cells were filtered through a 70-µm filter. The single cell suspension was harvested in ice-cold phosphate buffered saline (PBS) and incubated with the antibody (murine CD206, Biolegend 141708) in the darkroom for 30 min. Then, the stained cells were washed in PBS and stored at 4 °C prior to flow cytometric analysis (Accuri C6, BD, USA). For each analysis, an isotype matched monoclonal antibody was used as a negative control. Each experiment was performed three times.

Real-time reverse transcribed polymerase chain reaction (RT-PCR) and Western blotting

Real-time RT-PCR and Western blotting were routinely performed, as previously described [8]. Thirty-one genes were detected by real-time RT-PCR, and twenty-four genes were detected by Western blotting. The information of primers and antibodies is listed in supplementary material (Tables S2 and S3).

Immunocompetent murine PDAC models and chemotherapy in vivo

Thirty-five eight-week-old male C57BL/6 J mice were used for subcutaneous bearing model. A total of 2×10^6 Panc02 cells per mice were subcutaneously implanted. After 3 weeks, mice were allocated into 5 groups (7 mice/group): control, GEM, GEM+anti-TGF-β1, GEM+anti-GM-CSF and GEM+anti-TGF-β1/GM-CSF. The GEM was administered at 50 mg/kg, 2×/week intraperitoneal, antibodies against TGF-β1 (400 µg/kg, Abcam, No. ab92486) and/or GM-CSF (400 µg/kg, Abcam, No. ab9741) 2×/week intratumoral. The saline was used for control. Tumor volume was calculated as $0.5 \times \text{length} \times \text{width} \times \text{width}$ [8]. The treatment of GEM and antibodies continued for 4 weeks, and then, mice were sacrificed. The tumors were harvested and weighted. The tumor growth curve was compared in each group. The increased ratio of final tumor weight to initial tumor weight (initial tumor volume as representative of initial tumor weight) was calculated and compared in each group.

Liver metastasis model was established by intrasplenic injection of Panc02 cells (3×10^6/mouse). Two weeks after intrasplenic injection, GEM (100 mg/kg, intraperitoneal injection, twice per week) with or without combined blockade of TGF-β1/GM-CSF (200 µg/kg, intraperitoneal injection, twice per week) was used for 2 weeks. One month after intrasplenic injection, one cohort (16 mice) were sacrificed and the liver with metastatic lesions was weighted and compared. Another cohort (24 mice) were followed up till 2 months after intrasplenic injection, and the survival was compared.

Statistical analysis

IBM SPSS Statistics software 22.0 version and Graphpad prism software 5.0 version were used for statistical analysis and graphs (Version 5.0, Graph-Pad Software, La Jolla, CA, USA). The optimal cutoff values to predict OS were determined by the X-Tile program. Survival time was calculated using the Kaplan–Meier method. Univariate and multivariate analyses were based on log-rank test and Cox proportional hazards regression model. For analysis of the interconnections of variables of TIME, the Spearman coefficients test was used. For comparison of individual variables, the Student's *t* test (normal distribution data), the Mann–Whitney *U* test (non-normal distribution data) and the *Fisher's* exact tests were applied appropriately. The Tukey's range test was used for multiple repeated comparisons. Two-tailed $p \leq 0.05$ was judged to be significant.

Results

Patient cohort and demographic information

The follow-up time for living patients ranged from 31 to 93 months (median 55 months). The overall 1-year, 2-year and 3-year survival rates were 77.2%, 52.6% and 37.4%, respectively. The median age of the patients was 60 years, and there were 36 female and 61 male patients. A total of 74.4% of the tumors were larger than 2 cm in diameter. A total of 62.9% of the patients had lymph node metastasis. A total of 73.2% of the tumors were well or moderate differentiation. Serum CA-19-9, CA242 and CEA elevated in 71.1%, 38.1% and 19.5% of the patients, respectively. The detail of these 16 routine clinicopathological characters of this cohort is presented in Table S4.

Immune cells in tumor tissue

The high level (> 10/HPF) of infiltration of CD45 positive immune cells was found in 92.7% of the tumor tissues. There were massive CD45 positive immune cells in tumor tissue (59.6 ± 6.08/HPF). The infiltration of PD1 positive T cells, PDL1 positive stroma cells, IgG4 positive plasma cells, Foxp3 positive Treg cells, S-100 positive dendritic cells (DC) and CD56 positive natural killer cells (NK) were low level. The PD1 positive T cells were extremely rare (0.1 ± 0.57/core) and found only in 4.10% of the tumor tissues. Infiltration of the PDL-1 positive stroma cells was found in 80.4% of the tumor tissue; however, the number of PDL-1 positive stroma cells was also very low (3.37 ± 0.32/HPF). The Treg cells and IgG4 positive plasma cells were detected in 77.3% and 66.7% of the tumor tissues with a low number (3.21 ± 033/HPF, 3.21 ± 033/core, respectively). The number of the DC cells and the NK cells were also very low (2.02 ± 0.25/HPF and 2.73 ± 0.30/HPF, respectively) and found in 62.90% and 80.40% of the tumor tissues. The infiltrations of CD20 positive B lymphocytes, IgG positive plasma cells, CD15 positive granulocytes, CD4 positive helper T lymphocytes (Th) and CD8 positive cytotoxic T lymphocytes (CTLs) were moderate level, and they were found in 100% of the tumor tissues. CD3 positive T lymphocytes (24.39 ± 2.12/HPF) and CD68 positive TAM (37.56 ± 1.87/HPF) displayed high level of infiltration. The majority of TAM in tumor tissue was immunosuppressive CD163 positive M2-polarized TAM (30.73 ± 1.99/HPF) (Table S5) (Fig. 1).

Expressions of Th1/Th2 cytokines, GM/M-CSF, TGF-β1, IFN-γ and PDL-1 in PDAC cells

Among Th1/Th2 cytokines, IL6 and IL17 were expressed at low levels in all cases; however, IL4 and IL10 were much higher expressed in most cases. M-CSF was weakly expressed in the majority of the cases; in contrast, GM-CSF was moderately or strongly expressed in most of the cases. TGF-β1 has moderate and strong expression in most tumor tissue. TNF-α was moderately expressed in 3 cases and weakly in the remaining cases. Unexpectedly, IFN-γ was moderately expressed in 4 cases and strongly expressed in 17 cases. PDL-1 was weakly expressed in cancer cells of most of the cases, with moderate and strong expression in only 6 cases. FOXP3, which is regarded as the surrogate of Treg, was also found to be expressed in cancer cells, and it was moderately and strongly expressed in 34 cases (Figs. S3–S4).

Angiogenesis, lymphangiogenesis and PCSC in tumor tissue

The CD133 and ALDH1 positive PCSC were detected in 42.3% and 39.2% of cases, respectively (Fig. S5). The microvascular density (MVD) ranged from 5 to 50/HFP, and the median value was 19.0/HFP in tumor tissue. The number of microlymphatic vascular density (MLVD) was ranged from 1 to 48/HFP, and the median value was 8.0/HFP in tumor tissue (Fig. S6).

Identification of predictive factors for survival of the patients

The optimal cutoff values of each item to stratify the survival of the patients were defined by using X-tile program (Table S6). Among 46 factors (16 routine clinicopathological characters plus 30 items in TIME), univariate analysis identified 21 variables as potential prognostic factors for survival, including age, tumor size, lymph node metastasis, differentiation grade, the 8th TNM staging, CA19-9, CA242, CD45, CD3, CD4, CD8, CD15, CD163, IgG4, Treg, TGF-β1, GM-CSF, FOXP3 (tumoral), CD133, CD34 and D2-40 (Table S7). Further, the multivariate analysis further identified 8 items as independent risk factors for poor survival, including 3 clinicopathological characters, i.e., lymph node metastasis, poor differentiation, CA19-9 and 5 items in TIME, i.e., CD163, IgG4, TGF-β1, GM-CSF and D2-40 (Table 1, Fig. 2a–h). The area under curve (AUC) of the receiver operating curve (ROC) showed that the top three negative prognostic predictors for death in the TIME were CD163, CA19-9 and TGF-β1 (Fig. 2i and Fig. S8). The sensitivity and specificity of each item are presented in detail in the supplementary material (Table S8).

We further tested the roles of the combinations of the traditional independent risk factors (differentiation, CA19-9 and lymph node metastasis) and the TIME independent risk factors (CD163, IgG4, TGF-β1, GM-CSF and D2-40) to stratify the survival, respectively. The results showed that the patients with more traditional independent risk factors
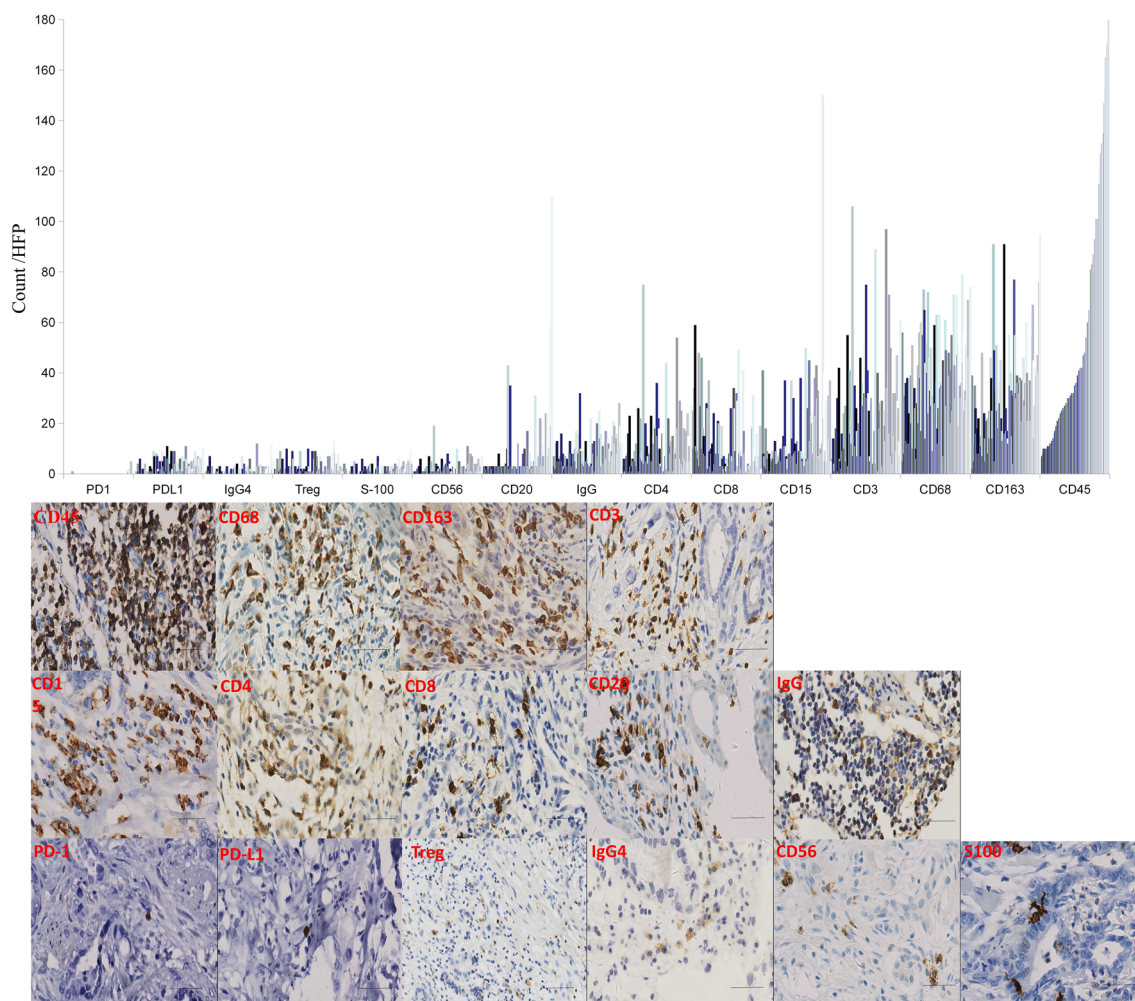
Fig. 1 IHC staining of immune cell populations in pancreatic cancer tissue: statistics of the infiltrations of 15 immune cell populations in 97 pancreatic cancer patients (upper panel); representative figures of IHC staining were shown (400×, magnification, low panel)

or TIME independent risk factors had worse survival, e.g., all of 11 patients who had no traditional independent risk factors survived during the follow-up period; however, the median survival of all of the 24 patients who had four or five TIME independent risk factors was only 12.0 m which was extremely poor. As well, the combination of TIME independent risk factors has substantial roles to further stratify the patients who have been stratified by traditional independent risk factor (Fig. S9, Table S9).

Interconnections of 21 risk factors correlated to survival of the PDAC patients

The interconnections of the risk factors correlated to poorer survival were analyzed by using Spearman coefficients test. Briefly, poorly differentiated tumors (G3) and

tumors larger than 4 cm expressed higher levels of TGF-β1 ($p < 0.01$, $p < 0.05$), respectively. High level of TGF-β1 was correlated with more infiltration of CD45 positive immune cells, CD15 positive granulocytes, Treg and M2-polarized TAM ($p < 0.01$, all). High level of TGF-β1 was also correlated with increased angiogenesis and more PCSCs ($p < 0.01$). High level of TGF-β1 paralleled GM-CSF levels ($p < 0.01$). High level of GM-CSF paralleled PCSCs ($p < 0.01$), Treg ($p < 0.05$) and tumor-expressing FOXP3 ($p < 0.01$). Tumor-expressing FOXP3 was correlated with lymphangiogenesis ($p < 0.05$). More infiltration of M2-polarized TAM paralleled CD45 positive immune cells, CD15 positive granulocytes and Tregs ($p < 0.01$, all). Therefore, M2-polarized TAM, TGF-β1 and GM-CSF were positively correlated with cancer stemness, angiogenesis and lymphangiogenesis (Table S10).

Table 1 Independent risk factors to predict poorer survival of the patients

Characters	No.	Univariate analysis			Multivariate analysis		
		Median ± SE	95%CI	P*	HR	95%CI	P#
LN metastasis				< 0.001	3.287	1.58–6.86	< 0.001
N0	37	55.00 ± 6.65	41.98–68.02				
N1-2	60	21.00 ± 2.90	15.31–26.69				
Grade				0.001	1.974	0.99–3.94	0.050
G1-2	71	40.00 ± 5.66	28.92–51.08				
G3	26	15.00 ± 0.55	10.00–20.00				
CA19-9				< 0.001	5.296	1.65–17.01	0.005
≤ 34U/ml	27	54.98 ± 6.77	41.71–68.26				
> 34U/ml	69	24.00 ± 3.12	17.90–30.11				
CD163				< 0.001	2.323	1.02–5.31	0.046
≤ 35/HPF	53	45.00 ± 7.09	31.11–58.90				
> 35/HPF	44	18.00 ± 1.65	14.76–21.24				
IgG4				< 0.001	3.758	1.48–9.56	0.005
≤ 2/core	41	55.00 ± 5.81	43.60–66.40				
> 2/core	56	18.00 ± 2.50	13.11–22.90				
TGF-β1				< 0.001	2.508	1.02–6.19	0.040
0–8	58	44.00 ± 10.79	22.85–65.15				
9–12	39	17.00 ± 1.56	13.94–20.06				
GM-CSF				0.016	2.254	0.91–5.58	0.049
0–8	31	40.00 ± 11.96	16.56–63.44				
9–12	66	24.00 ± 4.06	16.04–31.96				
D2-40(MLVD)				0.047	5.198	2.20–12.29	< 0.001
≤ 6/HPF	47	41.00 ± 5.16	30.88–51.12				
> 6/HPF	50	24.00 ± 5.30	13.61–34.39				

*Log-rank test

#COX regression test

Differential expression of the independent risk factors of TIME in tumoral and peritumoral tissues

The differential expressions of 5 independent risk factors in tumor and peritumoral tissue were analyzed. All peritumoral tissues displayed low expression of TGF-β1; in contrast, 85.6% of the tumor tissues had moderate or strong expression of TGF-β1 ($p < 0.001$). A total of 74.1% of peritumoral tissues had low-level expression of GM-CSF, whereas 78.3% of tumor tissue had moderate or strong expression of GM-CSF ($p < 0.001$). There were much more CD163 positive M2-polarized TAMs (21.39 ± 1.955/HPF versus 10.65 ± 1.082/HPF, $p < 0.001$) and IgG4 positive plasma cells (2.90 ± 0.61/core versus 1.41 ± 0.23/core, $p < 0.05$) in tumor tissues than in peritumoral tissues. The MLVD in tumor tissue was much higher, compared to that in peritumoral tissue (12.65 ± 1.1/HPF versus 4.36 ± 0.30/HPF) (Fig. 3).

TAM induced by PDAC cells weakened the efficacy of GEM

The PDAC cells were cultured in different conditional media and different concentrations (0.1, 1 and 10 µmol/l) of GEM were added for chemotherapy. The Annexin-V/PI method was used to detect the survival, apoptosis and necrosis of the cancer cells. The murine and human PDAC cells showed different sensitivity to GEM. When the survived cancer cells were compared, the SN from TAM substantially protects all of the different PDAC cells from chemocytotoxicity and decreased the efficacy of GEM (Fig. S10).
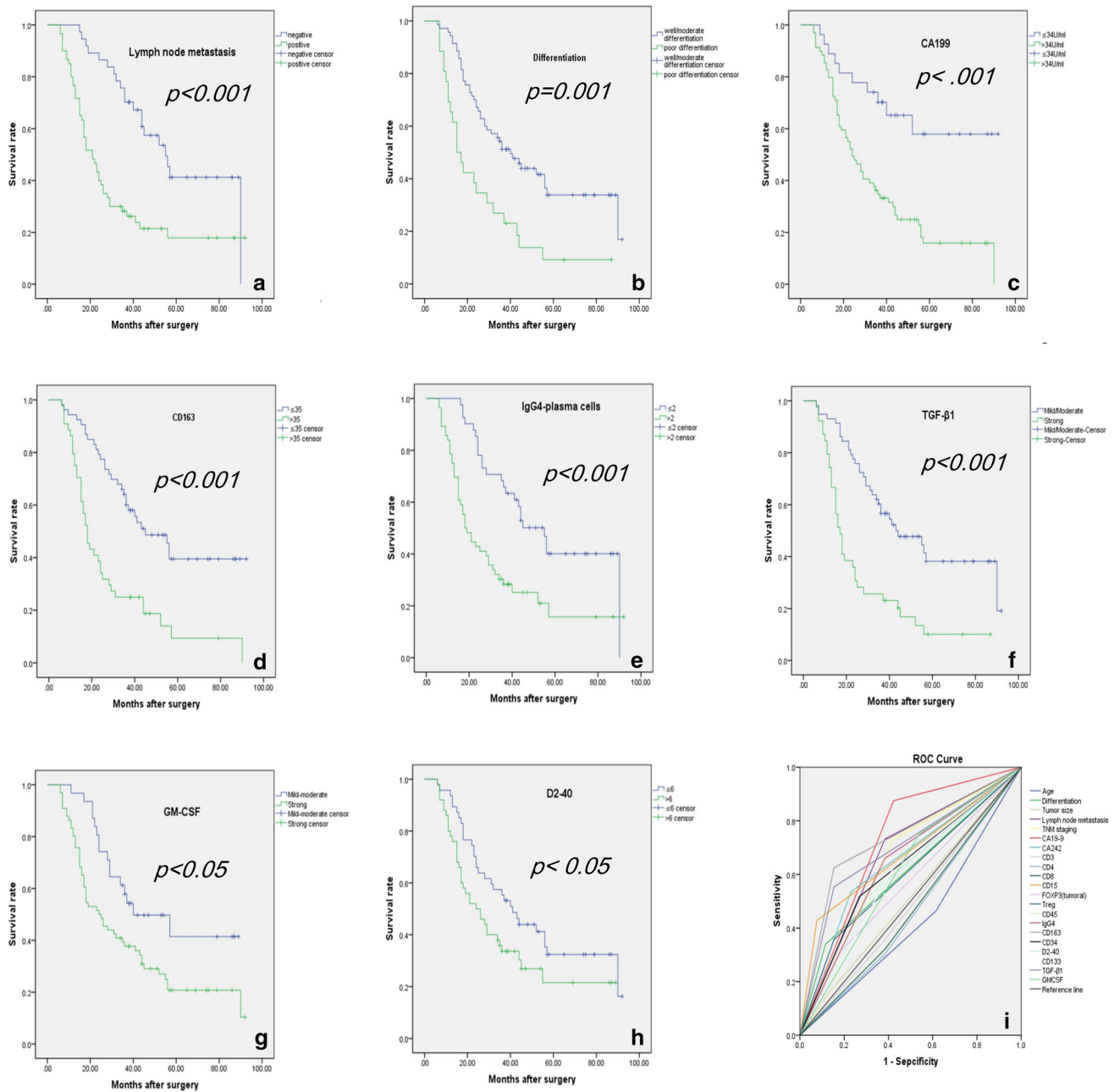
Fig. 2 Independent risk factors for the survival of the PDAC patients: **a** the positive lymph node metastasis predicted worse survival; **b** the poor differentiation predicted worse survival; **c** the elevated CA19-9 predicted worse survival; **d** the higher level of infiltration of CD163 positive M2-polarized TAM (> 35/HPF) predicted worse survival; **e** the higher level of infiltration of IgG4 positive plasma cells (> 2/core) predicted worse survival; **f** the strong positive expression of TGF-β1 in tumoral tissue predicted worse survival; **g** the strong positive expression of GM-CSF in tumoral tissue predicted worse survival; **h** the higher MLVD in tumoral tissue (> 6/HPF) predicted worse survival. **i** the ROC curve analysis showed that the top three values of AUC to predict death were CD163 positive M2 TAM, CA19-9 and TGF-β1

GEM could induce PDAC cells to express TGF-β1 and GM-CSF to induce M2-polarized TAM

The changes of IL4/6/10/17, GM-CSF, M-CSF, IFN-γ, TNF-α, FOXP3, CD 133, ALDH-1A of human and murine PDAC cells before and after GEM treatment at mRNA level and protein level were detected by real-time RT-PCR and Western blot in vitro. GM-CSF, IL-4, IL-6, IL-10, PDL-1, CD133 and FOXP3 had an increase trend after GEM treatment, and TGF-β1 and GM-CSF were significantly elevated in all of these 4 PDAC cancer cell lines at both mRNA and protein levels at all concentrations of

Fig. 3 Comparative expressions of independent risk factors of TIME in tumoral and peritumoral tissue: **a** the TGF-β1 had moderate or strong expression in most tumor tissue; however, there was only mild expression in peritumoral tissue (*Fisher's exact test*, ** $p < 0.01$); **b** the GM-CSF had much higher expression in tumor tissue, compared to that in peritumoral tissue (*Fisher's exact test*, **$p < 0.01$); **c** there were much more infiltration of M2-polarized TAM in tumor tissue, compared to that in peritumoral tissue (Mann–Whitney *U* test, ** $p < 0.01$). **d** There were much more infiltrations of IgG4 positive plasma cells in tumor tissue, compared to that in peritumoral tissue (Mann–Whitney *U* test, **$p < 0.01$); **e** the MLVD in tumor tissue was significantly higher than that in peritumoral tissue (Mann–Whitney *U* test, **$p < 0.01$)
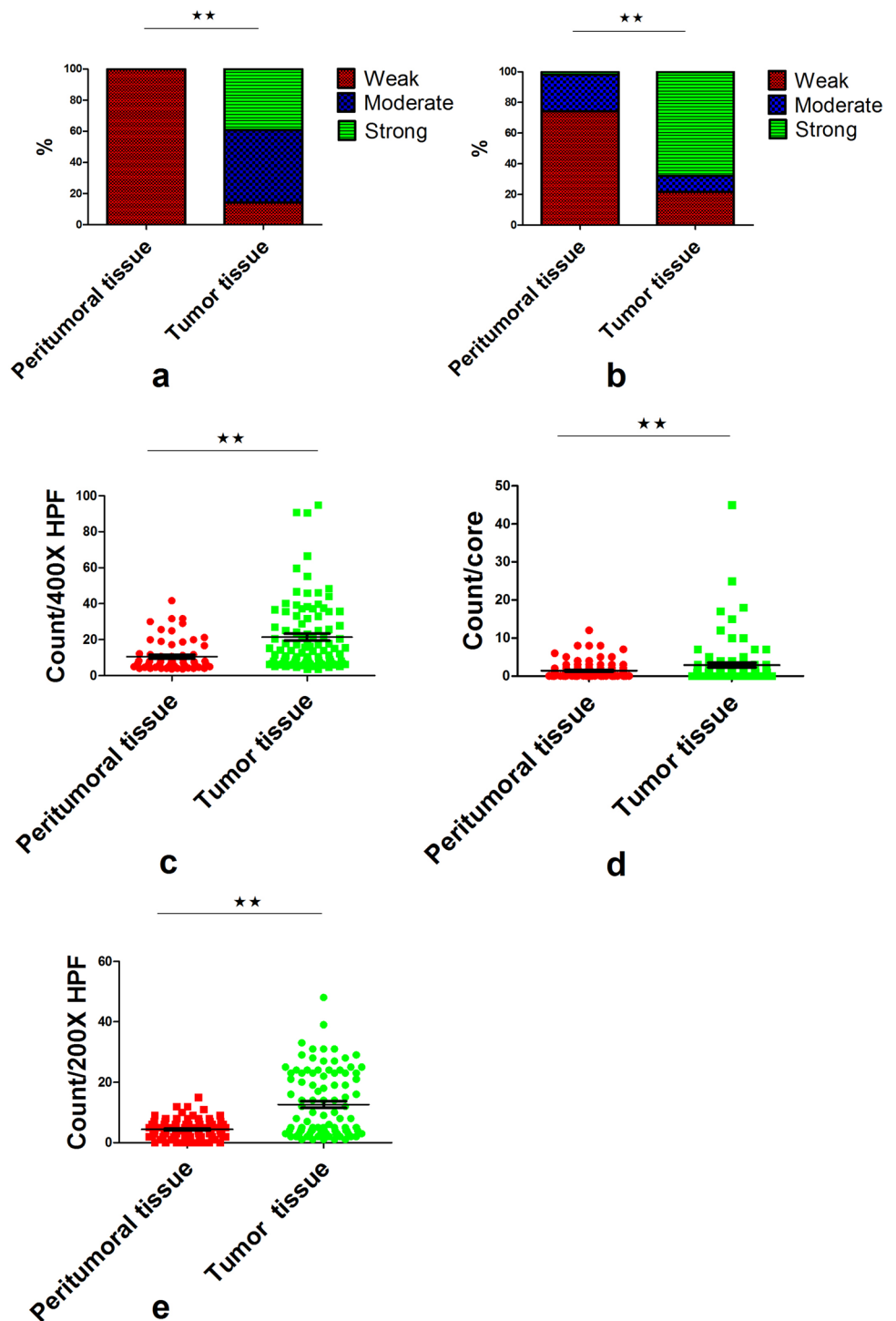
GEM with the highest increase (Fig. 4a, b). GEM treatment led to smaller tumor size in tumor subcutaneous bearing model. The HE staining also showed there was extensive necrosis in the tumor tissue after GEM treatment (Fig. 4c). The results of RT-PCR, Western blotting and IHC staining also confirmed that after GEM treatment, the Panc02 tumor tissue expressed higher level of TGF-β1 and GM-CSF (Fig. 4c, d).

Human (THP1) and murine monocyte cells (RAW264.7) were labeled by CFSE. The lipopolysaccharides (LPS) was used to induce M1 polarized macrophages. The M1 polarized macrophages showed a specific morphology with a round body, multiple intracellular vacuole and short and multiple pseudopodia; however, the TAM induced by SN of PDAC cells showed a morphology with a spindle-shaped body with oligo-long pseudopodia (Fig. S11). Both human
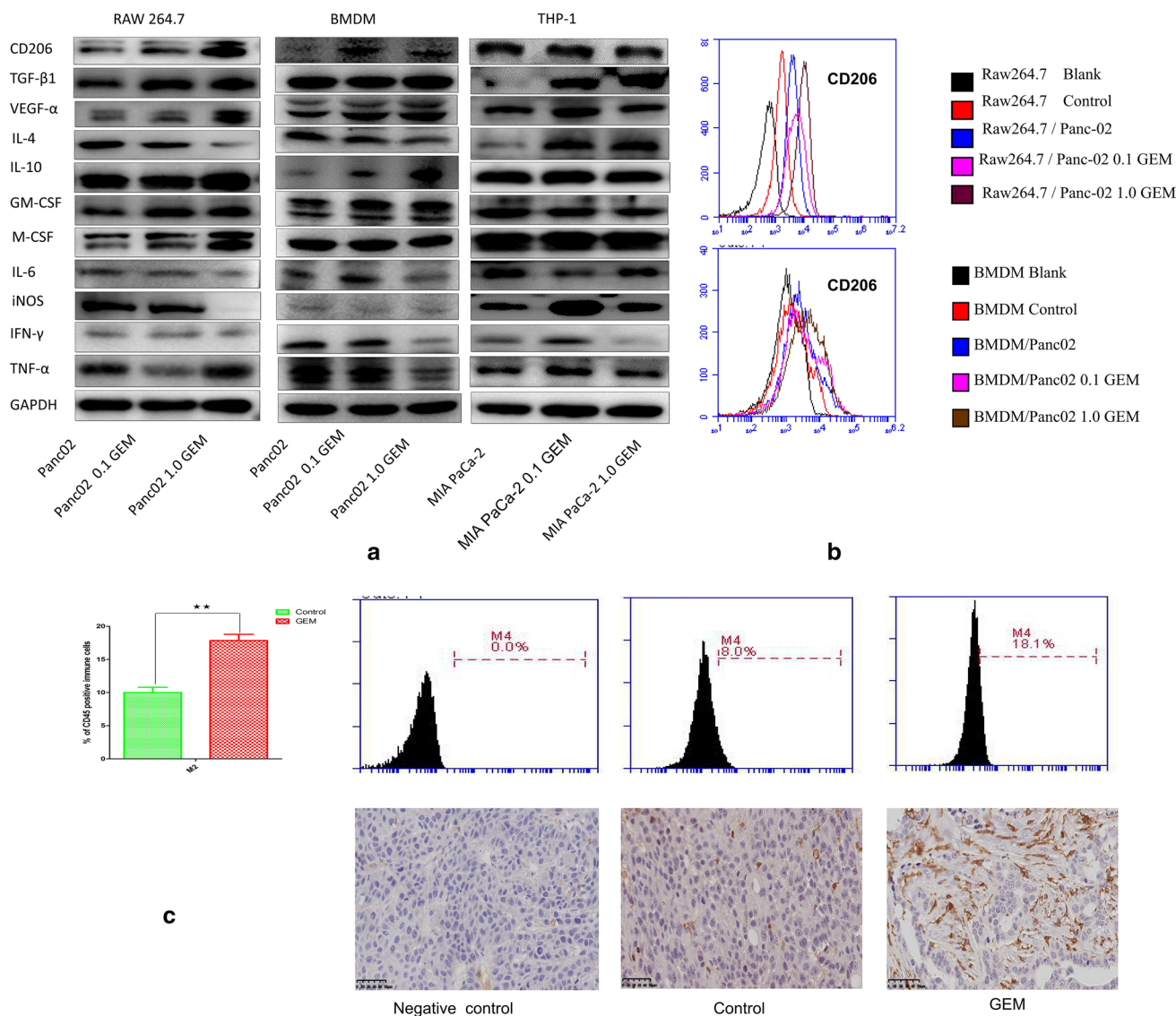
Fig. 4 GEM could induce pancreatic cancer cells to express higher level of TGF-β1 and GM-CSF both in vitro and in vivo: **a** after treatment of GEM at three different concentrations (0.1 μmol/L, 1.0 μmol/L, 25 μmol/L), many inflammatory factors were elevated; however, TGF-β1 and GM-CSF were elevated in all of these 4 PDAC cell lines and had the highest increase at mRNA level (Tukey's test,***$p < 0.001$, **$p < 0.01$, *$p < 0.05$, respectively); **b** the rep-resentative figures of Western blotting were shown; **c** GEM group had smaller tumor weight, and there was extensive necrosis in GEM group. Real-time RT-PCR and Western blotting showed that after GEM treatment, tumor tissue had a higher expression of TGF-β1 and GM-CSF, compared to control group; **d** the representative figures of IHC staining of TGF-β1 and GM-CSF were presented (200×, magnification)

and murine PDAC cells induced more M2 like TAM with spindle shape and oligo-long pseudopodia after GEM treatment (Fig. S12). Further, the murine GEM-treated PDAC cells (Panc02) induced more murine CD206 positive M2-polarized TAMs and higher expressions of the effector cytokines of M2-polarized TAM, including GM-CSF, M-CSF, TGF-β1 and VEGF-α levels (Fig. 5a, b). Although the GEM-treated human PDAC cells did not induce higher expression of CD163 or CD 206 in human TAM, the expression of effector cytokines of M2-polarized TAM, such as TGF-β1 and IL-4 in TAM were also elevated. After GEM

treatment, the CD206 positive M2 TAM in tumor tissue was detected by FCM and IHC. The results showed that after GEM treatment, the infiltration of M2 TAM in tumor tissue increased significantly (Fig. 5c).

Combined blockade of TGF-β1 and GM-CSF improved the efficacy of GEM by modulating the immunosuppressive TIME

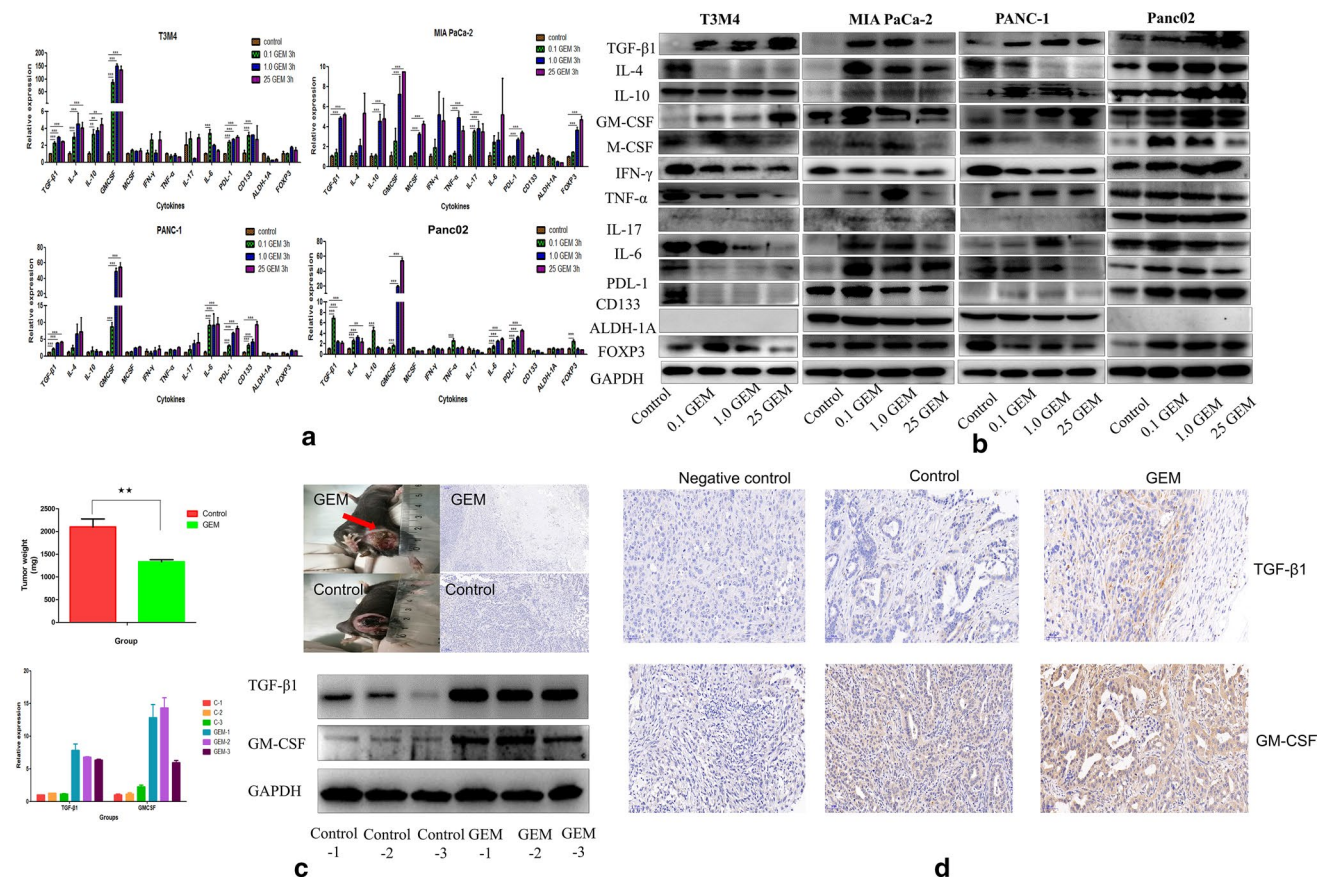According to our defined criteria, among 30 items in TIME, TGF-β1 and GM-CSF could be the potential optimal targets

Fig. 5 GEM-treated PDAC cells induced M2 polarization of TAM: **a**, **b** Western blotting and FCM results showed that after co-cultured with GEM-treated PDAC cells, murine RAW 264.7 cells, murine BMDM expressed higher level of M2 surface markers (CD206 and CD163) and M2 functional factors (GM-CSF, TGF-β1, VEGFA, IL10), to the contrary, M1 function factor (iNOS) was decreased.

Although human THP-1-drived TAM did not expressed higher level of M2 surface markers (CD206 and CD163), the M2 functional factors were also elevated (TGF-β1, IL4), and the M1 functional cytokine (IFN-γ) was decreased; **c** the FCM results showed that after GEM treatment, there were more M2-polarized TAM infiltrations (Student's *t* test, **$p < 0.01$). It was further confirmed by IHC

to improve the chemotherapeutic effects. In the immuno-competent murine subcutaneous bearing model, the tumor growth curve showed that GEM significantly inhibited the tumor growth, compared to the control group, and combined blockade of TGF-β1 and GM-CSF substantially improved the efficacy of GEM (Fig. 6a, b). When the increase-fold of tumor weight were compared, as well, GEM inhibited the growth of tumors, compared to control group (12.0 ± 1.3 versus 17.7 ± 3.2, $p < 0.05$). Antibodies against TGF-β1 or GM-CSF alone did not show significant effects (GEM versus GEM + anti-GM-CSF, 12.0 ± 1.3 versus 11.3 ± 1.9, $p > 0.05$; GEM versus GEM + anti-TGF-β1, 12.0 ± 1.3 versus 8.0 ± 1.2, $p > 0.05$). However, the combined use of anti-bodies against TGF-β1 and GM-CSF significantly improved the efficacy of GEM (GEM versus GEM + anti-TGF-β1 / GM-CSF, 12.0 ± 1.3 versus 6.1 ± 1.1, $p < 0.01$) (Fig. 6b, Fig. S13).

Similar to the in vitro studies, after GEM treatment, there was more infiltration of CD206 positive M2-polarized TAM

in tumor tissue (control versus GEM, 24.0 ± 1.2/HFP versus 38.7 ± 3.9/HFP, $p < 0.01$); however, combined blockade of TGF-β1 and GM-CSF significantly reduced M2-polarized TAM (control versus GEM+anti-TGF-β1 /GM-CSF, 24.0 ± 1.2/HFP versus 13.1 ± 1.5/HFP, $p < 0.01$) (Fig. 6c, Fig. S14). In contrast, there were less CD8 positive CTLs in tumor tissue after GEM treatment (control versus GEM, 9.7 ± 0.5/HFP versus 4.8 ± 1.0/HFP, $p < 0.01$); however, combined blockade of TGF-β1 and GM-CSF led to more infiltration of CD8 positive T cells (GEM versus GEM+anti-TGF-β1 /GM-CSF, 4.8 ± 1.0/HFP versus 8.1 ± 1.0/HFP, $p < 0.01$) (Fig. 6d and Fig. S15).

The mice treated by the combined regimen survived a significant longer time than the mice treated by GEM alone (Fig. 6e). The weight of liver with metastasis in GEM plus anti-TGF-β1 and GM-CSF group was less than that of GEM alone group (Fig. 6f and Fig. S16).

This novel combined blockade of TGF-β1 and GM-CSF significantly improved the chemotherapeutic effects by

Fig. 6 Combined blockade of TGF-β1 and GM-CSF improved the chemotherapeutic effects in immunocompetent murine PDAC models: **a** the tumor growth curve showed that the combined blockade regimen improved the effects of GEM; **b** the comparison of the tumor weight also showed that combined blockade of TGF-β1 and GM-CSF significantly improved the effects of GEM ($**p < 0.05$, Tukey's test); **c** after GEM treatment, there were more infiltrations of M2 TAM in tumor tissue ($**p < 0.01$); after combined blockade of TGF-β1 and GM-CSF, the accumulation of M2-polarized TAM was inhibited ($**p < 0.01$, Tukey's test); **d** after GEM treatment, there were less infiltration of CTL in tumor tissue ($p < 0.01$, Tukey's test); after combined blockade of TGF-β1 and GM-CSF, the infiltration of CD8 positive cells was restored ($**p < 0.01$);**e** combined blockade of TGF-β1 and GM-CSF plus GEM led to better survival than GEM alone for liver metastasis mice (median survival, 29 days vs 34 days, $*p < 0.05$, log rank test); **f** combined blockade of TGF-β1 and GM-CSF plus GEM led to less metastatic tumor burden than GEM alone (1690 ± 99.61 mg vs 975 ± 78.58 mg, $**p < 0.01$, t test)
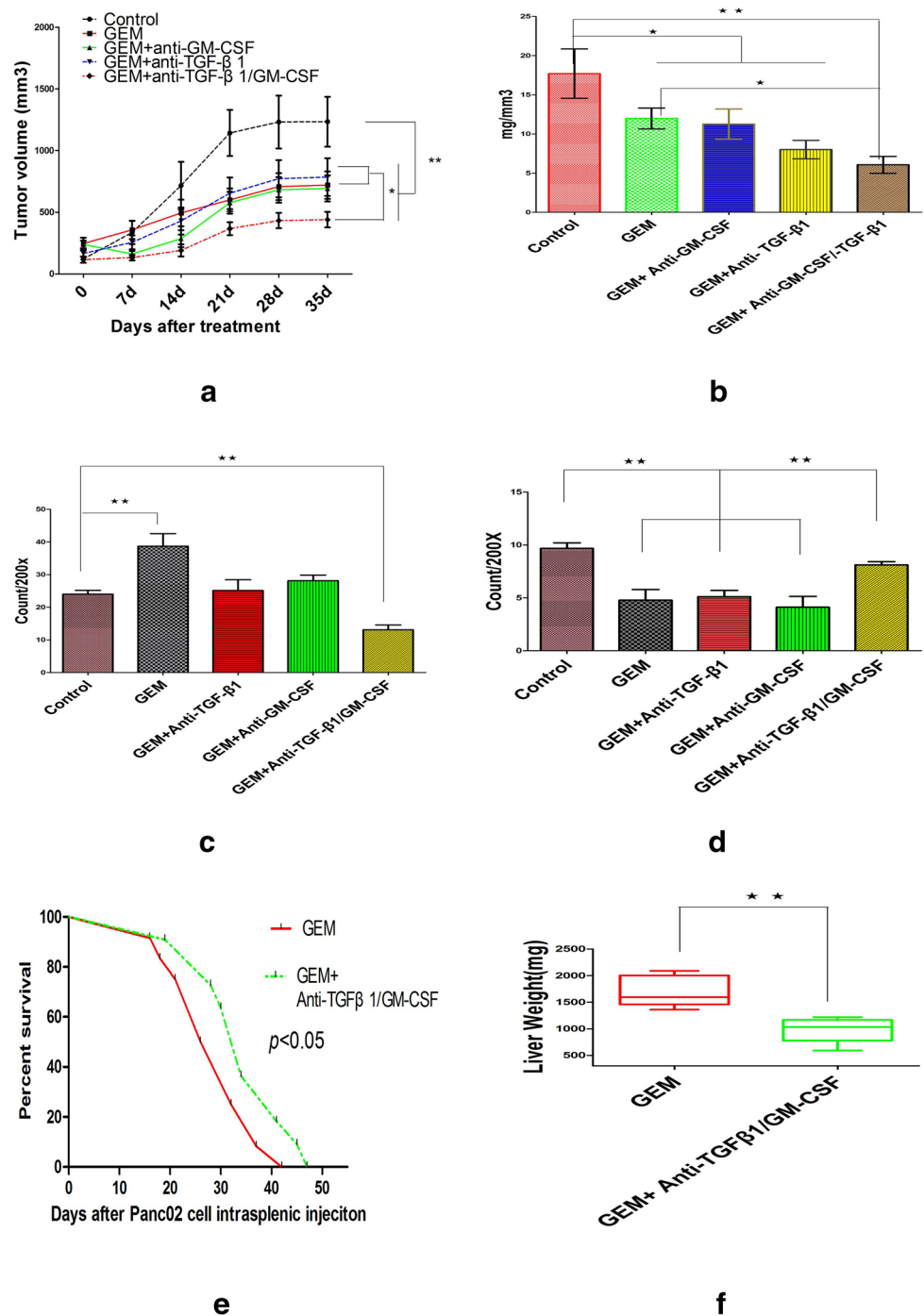
inhibition of M2 TAM and induction of CD8 positive T cell (Fig. S17).

Discussion

Surgical resection in combination with ACT is the standard treatment strategy for resectable pancreatic cancer; however, the prognosis of these patients is still not satisfactory. To develop new strategies in order to improve the efficacy of chemotherapy is important to prolong patient survival [4, 20, 21]. Immune regulatory factors produced by cancer cells weaken anti-tumor effects of immune cells, and then, these immune cells exert tumor-promoting effects via various mechanisms [3, 22–24]. Targeting the TIME may present a potential way to improve the effects of chemotherapy. However, the landscape of TIME has not been systematically depicted before. Here, we proposed that five aspects play

vital roles in TIME: immune cells, tumor cells producing immune regulatory factors, PCSC, angiogenesis and lymphangiogenesis. The first aim of this study was to delineate the TIME landscape and uncover their interconnections and their predictive roles for survival. Adjuvant chemotherapy has been demonstrated to improve the survival of PDAC patients after radical resection, and gemcitabine was the first line treatment before 2014 in our center. The resection margin also can affect the survival of the patient. Therefore, in this study, to avoid the potential confounding factors, we only enrolled PDAC patients after radical resection and undergoing gemcitabine-based adjuvant chemotherapy. None of the patients underwent neoadjuvant chemotherapy.

Firstly, a higher number of CD45 positive immune cells predicted worse survival of patients. Among all of these immune cell subpopulations, the number of TAM was the highest and most of them expressed M2 markers; however, CD4 and CD8 positive T cells were observed less frequently. Mahajan et al. [25] found that CD3, CD4, CD8 positive T cells were independently associated with tumor recurrence by using 1824 tissue microarray specimens from 385 patients. We also found that higher infiltration of CD 3, CD4, CD8 positive T cells predicted better OS. However, after multivariate analysis by using all 21 risk factors, they were not independent risk factors in this study. It has been reported that due to the lack of specific tumor antigens and the immunosuppressive microenvironment, T cells cannot be activated to kill cancer cells [26]. Several previous studies showed that immune checkpoint inhibitors did not improve the survival of the pancreatic cancer patients [27, 28]. In this study, we found the positive rate of PD1 positive T cells only at 4.1%, and the PDL-1 was negative or weak expression in 91 of 97 tumor tissues, which may partially explain the failure of inhibitors of immune checkpoint for pancreatic cancer. It has been reported that more infiltration of M2 predicted poorer survival of several cancers [8, 10, 25]. The CD163 positive M2-polarized TAM was also found to be an independent risk factor for worse survival in this study. The combination of an agonist CD40 antibody with GEM significantly increased the efficacy of GEM for pancreatic cancer by activation of macrophages, but not of T cells [14]. Thus, activation of TAMs, not T cells may be more effective to improve the efficacy of chemotherapy [14]. The NK cells and DC cells were reported to play important roles against several cancers [29], however, herein, the number of NK and DC cells was very small and they were not correlated with the survival of the patients. Previously, we reported that IgG4 positive plasma cells were independent factors for poor survival [8]; in this study, we further confirmed this result. Tregs and CD15 positive granulocytes also predicted poorer survival; however, after multivariate analysis, among all of the immune cells, only M2 positive TAMs and IgG4 positive plasma cells were independent risk factors for worse

survival. As well, we found that the SN from PDAC-induced TAM expressed higher levels of M2 type markers and effectors, leading to drug resistance.

Interestingly, we found that 34 of 97 tumor tissues expressed moderate or high level of FOXP3 which was regarded as a surrogate marker for Tregs [30]. We also found that higher levels of tumor-derived FOXP3 predicted worse survival. High expression of IL4 and IL10 could potentially induce M2-polarized TAM [31]; however, we did not find their correlation with patient survival in this study. Although M-CSF was reported to induce tumor-promoting macrophages [32, 33], in this study, we found that only very few tumors expressed high level of M-CSF. Among all 11 factors correlated to TIME produced by PDAC cells, multivariate analysis showed that only GM-CSF and TGF-β1 were independent risk factors for worse survival. The GM-CSF could exert effects on tumors in an immune-dependent manner [34, 35]. Bayne et al. [36] used a genetically engineered KRAS mutated murine model of pancreatic cancer and found that tumor-derived GM-CSF was necessary and sufficient to recruit immunosuppressive myeloid cells into tumor tissue. The whole-genome sequencing analyses showed that the common co-mutations detected in pancreatic cancer are SMAD4, KRAS, TP53 and CDKN2A [37]. Smad4 is a central mediator in the TGF-β signaling, and its inactivation can lead to the cooperation of KLF5 and SOX4 to promote tumorigenesis of pancreatic cancer [38]. TGF-β1 through Activin/Nodal activation is required for self-renewal and tumorigenicity of PCSC [39]. The TGF-β1 can also induce macrophages to M2-polarized TAMs to promote tumor growth by several mechanisms [3]. Herein, the correlation analysis also showed that TGF-β1 was positively correlated with M2-polarized TAM and PCSC.

The CD133 and ALDH1 were used as markers for cancer stem cells of several types of cancers, including pancreatic cancer [40]. Hermann et al. [41] found that human pancreatic cancer tissues contain cancer stem cells defined by CD133 that are tumorigenic and highly resistant to chemotherapy. We found a rate of CD133 and ALDH1 with 39.2 and 42.3% in tumor tissues, respectively. However, only CD133 correlated with patient survival. The expression levels of GM-CSF and TGF-β1 and infiltration of M2-polarized TAM were correlated with CD133 positive PCSC. It has been reported that M2-polarized TAMs potentially induce angiogenesis and lymphangiogenesis by secreting VEGF to promote metastasis of pancreatic cancer [3, 42]. In this study, more infiltrations of M2-polarized TAM were correlated with more angiogenesis. Further, lymphangiogenesis was correlated with tumor-producing FOPX3 and angiogenesis was related to Tregs. Several studied reported that M2-polarized macrophages could induce Tregs [43]. Univariate analysis found 21 risk factors correlated to worse survival of the patients; however, further multivariate analysis identified

only 8 independent risk factors, 5 of which are characters in TIME, i.e., IgG4 positive plasma cells, lymphangiogenesis, M2-polarized TAM, GM-CSF and TGF-β1, and all of them had a much higher expression level in tumor tissue, compared to peritumoral tissue. The results of the combinations of independent risk factors showed the patients had more independent risk factor had worse survival and the patients who had four or five TIME independent risk factors had an extremely poor survival with a median survival of 12 m and the combination of TIME factors can further stratify the patients who had been stratified by traditional factors. Therefore, the TIME items can improve the predictive roles of traditional items. The number of IgG4 positive plasma cells was very low which dwarfed its potential therapeutic roles, and the lymphangiogenesis is the outcome induced by tumor-promoting factors; therefore, M2-polarized TAM, GM-CSF and TGF-β1 might be optimal potential targets, after scanning of all of these 30 characters in TIME.

The mechanisms of drug resistance after chemotherapy treatment remain largely unknown. The possible roles of TIME in regulation of drug resistance have been gained more and more concerns. After paclitaxel and doxorubicin treatment in PyMT-MMTV mammary carcinoma, increased recruitment of TAM was found to be mediated by increased M-CSF [44]. After treatment with cisplatin and carboplatin, the expression of IL-6 was elevated in 10 gynecologic malignant cancer cell lines to induce M2-polarized TAM [45]. In this study, we tested three human and murine cell line by three different concentrations of GEM. Interestingly, in all 4 cell lines and at all concentrations of GEM, only the expression of TGF-β1 and GM-CSF was elevated in all PDAC cell lines. Further, after GEM treatment, PDAC cells showed much stronger potential to induce M2-polarized TAM. In a KRAS mutated murine pancreatic cancer model, GEM also induced recruitment of immature myeloid cells by increasing GM-CSF which dampened the chemotherapeutic effects [46].

Based on the above results, we proposed that intratumoral blockade of TGF-β1 and GM-CSF might improve the therapeutic efficacy by modulating of the TIME of PDAC. By using an immunocompetent murine subcutaneous PDAC bearing model and liver metastasis model, we found that combined blockade of TGF-β1 and GM-CSF, rather than any single target blockade, significantly improved the efficacy of GEM to inhibit tumor growth and to prolong the survival by inhibition of M2-polarized TAM and induction of CD8 positive T cells.

In this study, we mainly focused on the immune reaction in PDAC; however, we have to say that fibrosis which is caused mainly by fibroblast and pancreatic stellate cells is another character of PDAC which has been reported to affect chemotherapeutic effects and has interactions with immune cells. As well, PDAC is a highly heterogeneic tumor, and the genetic or epigenetic alterations of pancreatic cancer cells may determine the immune cell infiltration and fibrosis. Further studies are needed to uncover the molecular mechanisms of the network consisting of immune cells, fibrosis and genetic or epigenetic alteration of pancreatic cancer cells.

Conclusions

In this study, we comprehensively screened the TIME of PDAC patients and systematically analyzed their interconnections, survival impact and its reciprocal interactions with chemotherapy. Among 30 items, TGF-β1 and GM-CSF were proposed as the potential targets to improve chemotherapeutic roles. We further demonstrated that combined blockade of TGF-β1 and GM-CSF improved the effects of GEM by modulating the TIME. This novel combination strategy is promising to potentially improve the survival of the PDAC patients in the future.

Compliance with ethical standards

Conflict of interest All of the authors declared there was no conflict of interest.

Ethical approval and ethical standards This study was a retrospective study and was approved by the Ethics Committee of Peking Union Medical College Hospital and was registered at ClinicalTrials.org (NCT02654288).

Informed consent All of the patients signed the informed consent to donate samples for scientific research. In this study, only resected tumor and peritumor sample were used; therefore, there were nearly no potential harms to the patients.

Human and animal rights Male 4-week-old or 8-week-old C57BL/6 J mice were purchased from VITAL RIVER Animal Center (Beijing, China). Animal studies were performed in accordance with the institutional guidelines of Peking Union Medical College Hospital and was

approved by animal study committee of Peking Union Medical College Hospital on December 1, 2014.

Cell line authentication All cell lines were purchased from Cell Line Bank of Chinese Academy of Medicine Sciences.

References

1. Siegel RL, Miller KD, Jemal A (2018) Cancer statistics, 2018. CA Cancer J Clin 68:7–30
2. Wu WM, Jin G, Wang CY et al (2019) The current surgical treatment of pancreatic cancer in China a national wide cross-sectional study. J Pancreatol 2:16–21
3. Liu Q, Liao Q, Zhao Y (2017) Chemotherapy and tumor microenvironment of pancreatic cancer. Cancer Cell Int 17:68
4. Neoptolemos JP, Palmer DH, Ghaneh P et al (2017) Comparison of adjuvant gemcitabine and capecitabine with gemcitabine monotherapy in patients with resected pancreatic cancer (ESPAC-4): a multicentre, open-label, randomised, phase 3 trial. Lancet 389:1011–1024
5. Neesse A, Algul H, Tuveson DA et al (2015) Stromal biology and therapy in pancreatic cancer: a changing paradigm. Gut 64:1476–1484
6. Kleeff J, Korc M, Apte M et al (2016) Pancreatic cancer. Nat Rev Dis Primers 2:16022
7. Burkholder B, Huang RY, Burgess R et al (2014) Tumor-induced perturbations of cytokines and immune cell networks. Biochim Biophys Acta 1845:182–201
8. Liu Q, Li Y, Niu Z et al (2016) Atorvastatin (Lipitor) attenuates the effects of aspirin on pancreatic cancerogenesis and the chemotherapeutic efficacy of gemcitabine on pancreatic cancer by promoting M2 polarized tumor associated macrophages. J Exp Clin Cancer Res 35:33
9. Clark CE, Hingorani SR, Mick R et al (2007) Dynamics of the immune reaction to pancreatic cancer from inception to invasion. Cancer Res 67:9518–9527
10. Hou YC, Chao YJ, Hsieh MH et al (2019) Low CD8+ T cell infiltration and High PD-L1 expression are associated with level of CD44+/CD133+ cancer stem cells and predict an unfavorable prognosis in pancreatic cancer. Cancers (Basel) 11:E541
11. D'Costa Z, Jones K, Azad A et al (2017) Gemcitabine-induced TIMP1 attenuates therapy response and promotes tumor growth and liver metastasis in pancreatic cancer. Cancer Res 77:5952–5962
12. De Palma M, Lewis CE (2013) Macrophage regulation of tumor responses to anticancer therapies. Cancer Cell 23:277–286
13. Noy R, Pollard JW (2014) Tumor-associated macrophages: from mechanisms to therapy. Immunity 41:49–61
14. Beatty GL, Chiorean EG, Fishman MP et al (2011) CD40 agonists alter tumor stroma and show efficacy against pancreatic carcinoma in mice and humans. Science 331:1612–1616
15. Li C, Heidt DG, Dalerba P et al (2007) Identification of pancreatic cancer stem cells. Cancer Res 67:1030–1037
16. Baghdadi M, Wada H, Nakanishi S et al (2016) Chemotherapy-induced IL34 enhances immunosuppression by tumor-associated macrophages and mediates survival of chemoresistant lung cancer cells. Cancer Res 76:6030–6042
17. Gao Q, Qiu SJ, Fan J et al (2007) Intratumoral balance of regulatory and cytotoxic T cells is associated with prognosis of hepatocellular carcinoma after resection. J Clin Oncol 25:2586–2593
18. Chang W, Gao X, Han Y et al (2014) Gene expression profiling-derived immunohistochemistry signature with high prognostic value in colorectal carcinoma. Gut 63:1457–1467
19. Camp RL, Dolled-Filhart M, Rimm DL (2004) X-tile: a new bio-informatics tool for biomarker assessment and outcome-based cut-point optimization. Clin Cancer Res 10:7252–7259
20. The Lancet Gastroenterology H (2017) Pancreatic cancer: how can we tackle the lack of progress? Lancet Gastroenterol Hepatol 2:73
21. Ter Veer E, van Rijssen LB, Besselink MG et al (2018) Consensus statement on mandatory measurements in pancreatic cancer trials (COMM-PACT) for systemic treatment of unresectable disease. Lancet Oncol 19:e151–e160
22. Joyce JA, Fearon DT (2015) T cell exclusion, immune privilege, and the tumor microenvironment. Science 348:74–80
23. Bronte V, Murray PJ (2015) Understanding local macrophage phenotypes in disease: modulating macrophage function to treat cancer. Nat Med 21:117–119
24. Nielsen SR, Quaranta V, Linford A et al (2016) Macrophage-secreted granulin supports pancreatic cancer metastasis by inducing liver fibrosis. Nat Cell Biol 18:549–560
25. Mahajan UM, Langhoff E, Goni E et al (2018) Immune cell and stromal signature associated with progression-free survival of patients with resected pancreatic ductal adenocarcinoma. Gastroenterology 155:1625–1639
26. Posey AD Jr, Schwab RD, Boesteanu AC et al (2016) Engineered CAR T cells targeting the cancer-associated Tn-glycoform of the membrane mucin MUC1 control adenocarcinoma. Immunity 44:1444–1454
27. Topalian SL, Hodi FS, Brahmer JR et al (2012) Safety, activity, and immune correlates of anti-PD-1 antibody in cancer. N Engl J Med 366:2443–2454
28. Ning P, Lou WH, Jun Y (2019) PD-1 immunotherapy in pancreatic cancer. J Panreatol 2:6–10
29. Gurlevik E, Fleischmann-Mundt B, Brooks J et al (2016) Administration of gemcitabine after pancreatic tumor resection in mice induces an antitumor immune response mediated by natural killer cells. Gastroenterology 151(338–350):e7
30. Hinz S, Pagerols-Raluy L, Oberg HH et al (2007) Foxp3 expression in pancreatic carcinoma cells as a novel mechanism of immune evasion in cancer. Cancer Res 67:8344–8350
31. Casella G, Garzetti L, Gatta AT et al (2016) IL4 induces IL6-producing M2 macrophages associated to inhibition of neuro-inflammation in vitro and in vivo. J Neuroinflammation 13:139
32. Van Overmeire E, Stijlemans B, Heymann F et al (2016) M-CSF and GM-CSF receptor signaling differentially regulate monocyte maturation and macrophage polarization in the tumor microenvironment. Cancer Res 76:35–42
33. Ries CH, Cannarile MA, Hoves S et al (2014) Targeting tumor-associated macrophages with anti-CSF-1R antibody reveals a strategy for cancer therapy. Cancer Cell 25:846–859
34. Harris RJ, Pettitt AR, Schmutz C et al (2000) Granulocyte-macrophage colony-stimulating factor as an autocrine survival factor for mature normal and malignant B lymphocytes. J Immunol 164:3887–3893
35. Hong IS (2016) Stimulatory versus suppressive effects of GM-CSF on tumor progression in multiple cancer types. Exp Mol Med 48:e242
36. Bayne LJ, Beatty GL, Jhala N et al (2012) Tumor-derived granulocyte-macrophage colony-stimulating factor regulates myeloid inflammation and T cell immunity in pancreatic cancer. Cancer Cell 21:822–835
37. Neoptolemos JP, Kleeff J, Michl P et al (2018) Therapeutic developments in pancreatic cancer: current and future perspectives. Nat Rev Gastroenterol Hepatol 15:333–348
38. Ahmed S, Bradshaw AD, Gera S et al (2017) The TGF-beta/Smad4 signaling pathway in pancreatic carcinogenesis and its clinical significance. J Clin Med 6:5

39. Abel EV, Simeone DM (2013) Biology and clinical applications of pancreatic cancer stem cells. Gastroenterology 144:1241–1248

40. Kreso A, Dick JE (2014) Evolution of the cancer stem cell model. Cell Stem Cell 14:275–291

41. Hermann PC, Huber SL, Herrler T et al (2007) Distinct populations of cancer stem cells determine tumor growth and metastatic activity in human pancreatic cancer. Cell Stem Cell 1:313–323

42. Riabov V, Gudima A, Wang N et al (2014) Role of tumor associated macrophages in tumor angiogenesis and lymphangiogenesis. Front Physiol 5:75

43. Schmidt A, Zhang XM, Joshi RN et al (2016) Human macrophages induce CD4(+)Foxp3(+) regulatory T cells via binding and re-release of TGF-beta. Immunol Cell Biol 94:747–762

44. Hughes R, Qian BZ, Rowan C et al (2015) Perivascular M2 macrophages stimulate tumor relapse after chemotherapy. Cancer Res 75:3479–3491

45. Poth KJ, Guminski AD, Thomas GP et al (2010) Cisplatin treatment induces a transient increase in tumorigenic potential associated with high interleukin-6 expression in head and neck squamous cell carcinoma. Mol Cancer Ther 9:2430–2439

46. Takeuchi S, Baghdadi M, Tsuchikawa T et al (2015) Chemotherapy-derived inflammatory responses accelerate the formation of immunosuppressive myeloid cells in the tissue microenvironment of human pancreatic cancer. Cancer Res 75:2629–2640

Publisher's Note Springer Nature remains neutral with regard to jurisdictional claims in published maps and institutional affiliations.

Affiliations

Qiaofei Liu[1,3,4] · Huanwen Wu[2,3,4] · Yuan Li[2,3,4] · Ronghua Zhang[1,3,4] · Jorg Kleeff[5] · Xiang Zhang[1,3,4] · Ming Cui[1,3,4] · Jingkai Liu[1,3,4] · Tong Li[1,3,4] · Junyi Gao[1,3,4] · Boju Pan[2,3,4] · Wenming Wu[1,3,4] · Weibin Wang[1,3,4] · Li Zhou[1,3,4] · Junchao Guo[1,3,4] · Menghua Dai[1,3,4] · Taiping Zhang[1,3,4] · Quan Liao[1,3,4] · Zhaohui Lu[2,3,4] · Yupei Zhao[1,3,4]

1   Department of General Surgery, Peking Union Medical College Hospital, Peking Union Medical College and Chinese Academy of Medical Sciences, Beijing 100730, China

2   Department of Pathology, Peking Union Medical College Hospital, Peking Union Medical College and Chinese Academy of Medical Sciences, Beijing 100730, China

3   Department of Medicine, Tsinghua University, No. 1, Shuai Fu Yuan, Dong Chen District, Beijing 100730, China

4   National Translational Medicine Center, Peking Union Medical College Hospital, Peking Union Medical College and Chinese Academy of Medical Sciences, Beijing 100730, China

5   Department of Visceral, Vascular and Endocrine Surgery, Martin Luther University Halle-Wittenberg, 06108 Halle (Saale), Saxony-Anhalt, Germany